

# Supporting Information

## **Insight into the Charge Transfer Behavior of an Electrochemiluminescence Sensor Based on Porphyrin–Coumarin Derivatives with Donor–Acceptor Configuration**

Hui Xiao<sup>#</sup>, Yali Wang<sup>#</sup>, Yaqi Zhao<sup>#</sup>, Rongfang Zhang, Kainan Kang, Yanjun Feng, Yuling Gao, Huixia Guo, Bingzhang Lu<sup>\*</sup>, Peiyao Du<sup>\*</sup>, Xiaoquan Lu<sup>\*</sup>

*Key Laboratory of Water Security and Water Environment Protection in Plateau Intersection (Ministry of Education), Key Laboratory of Bioelectrochemistry & Environmental Analysis of Gansu Province, College of Chemistry & Chemical Engineering, Northwest Normal University, Lanzhou 730070, P. R. China*

*School of Chemical Engineering and Technology, Xi'an Jiaotong University, Shanxi 710049, P. R. China*

<sup>#</sup> These authors contributed equally to this work.

## Table of contents

### EXPERIMENTAL SECTION

Chemicals and materials

Synthesis of 5-(4-aminophenyl)-10,15,20-triphenyl porphine (ATPP)

Synthesis of diphenyl malonate (1)

Synthesis of 7-diethylamino-4-hydroxycoumarin (2)

Synthesis of 4-chloro-7-diethylaminocoumarin-3-aldehyde (3)

Synthesis of ATPP-Cou

Electrochemistry and ECL detection

IMPS and SPECM measurement

### FIGURE

**Scheme S1.** Preparation of ATPP.

**Scheme S2.** Preparation of diphenyl malonate.

**Scheme S3.** Preparation of 7-diethylamino-4-hydroxycoumarin.

**Scheme S4.** Preparation of 4-chloro-7-diethylaminocoumarin-3-aldehyde.

**Scheme S5.** Preparation of ATPP-Cou.

**Figure S1.** The  $^1\text{H}$  NMR spectrum of TPP ( $\text{CDCl}_3$ ).

**Figure S2.** The  $^1\text{H}$  NMR spectrum of 7-diethylamino-4-hydroxycoumarin ( $\text{DMSO-}D_6$ ).

**Figure S3.** The  $^1\text{H}$  NMR spectrum of 4-chloro-7-diethylaminocoumarin-3-aldehyde ( $\text{CDCl}_3$ ).

**Figure S4.** The  $^{13}\text{C}$  NMR spectrum of 4-chloro-7-diethylaminocoumarin-3-aldehyde ( $\text{CDCl}_3$ ).

**Figure S5.** The mass spectrum (ESI) of 4-chloro-7-diethylaminocoumarin-3-aldehyde.

**Figure S6.** The  $^1\text{H}$  NMR spectrum of 5-(4-aminophenyl)-10,15,20-triphenylporphyrin (ATPP) ( $\text{CDCl}_3$ ).

**Figure S7.** The  $^{13}\text{C}$  NMR spectrum of 5-(4-aminophenyl)-10,15,20-triphenylporphyrin (ATPP) ( $\text{CDCl}_3$ ).

**Figure S8.** The mass spectrum (ESI) of 5-(4-aminophenyl)-10,15,20-triphenylporphyrin (ATPP).

**Figure S9.** The  $^1\text{H}$  NMR spectrum of ATPP-Cou ( $\text{CDCl}_3$ ).

**Figure S10.** The  $^{13}\text{C}$  NMR spectrum of ATPP-Cou ( $\text{CDCl}_3$ ).

**Figure S11.** The mass spectrum (ESI) of ATPP-Cou. MS:  $m/z = 855.34$   $[\text{M-Cl}]^+$ .

**Figure S12.** CV curves of the bare GCE in PBS with (purple line) and without (navy-blue line)  $\text{K}_2\text{S}_2\text{O}_8$ .

**Figure S13.** Effect of different experimental conditions on the ECL system: (a) different potential windows, (b) different scan rates, (c) different concentrations of  $\text{K}_2\text{S}_2\text{O}_8$ , and (d) different pH values.

**Figure S14.** ECL intensity of the studied systems (bare GCE, Coumarin, ATPP and ATPP-Cou).

### TABLE

**Table S1.**  $K_{\text{eff}}$  values of different samples

**Table S2.** Transit time values of different samples

**Table S3.** The fluorescence lifetime fitting data of coumarin, ATPP and ATPP-Cou

**Table S4.** Comparison of the reported methods for  $\text{Cu}^{2+}$  detection

**Table S5.** Spiked recovery tests for river water samples

### REFERENCES

## EXPERIMENTAL SECTION

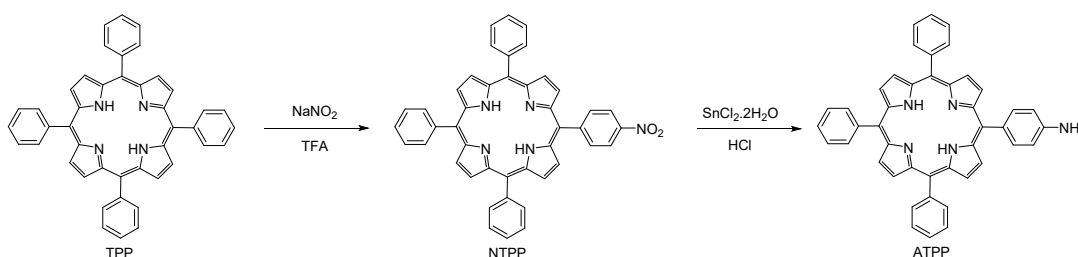
### Chemicals and materials

N, N-dimethylformamide (DMF, 99.9%), potassium chloride (KCl, 99%), potassium persulfate ( $K_2S_2O_8$ ,  $\geq 99.5\%$ ), potassium dihydrogen phosphate dihydrate ( $KH_2PO_4 \cdot 2H_2O$ ,  $\geq 99\%$ ), potassium hydrogen phosphate ( $K_2HPO_4$ , anhydrous,  $\geq 99\%$ ), copper chloride dihydrate ( $CuCl_2$ , 99%), zinc chloride ( $ZnCl_2$ , 99%), aluminum chloride ( $AlCl_3$ , 99%), cadmium chloride ( $CdCl_2$ , 99%), sodium chloride (NaCl, 99%), ferric chloride ( $FeCl_3$ , 99%), magnesium chloride ( $MgCl_2$ , 99%), cobalt nitrate hexahydrate ( $Co(NO_3)_2 \cdot 6H_2O$ , 99%), manganese chloride ( $MnCl_2$ , 99%), chromium sulfate ( $Cr_2(SO_4)_3$ , 99%), potassium ferricyanide ( $K_3[Fe(CN)_6]$ , 99%) and potassium ferrocyanide ( $K_4[Fe(CN)_6]$ , 99%) were obtained from Yantai Shuangshuang Chemical Co., Ltd. (Shandong, China). All the chemicals were employed as received without any purification.  $^1H$  NMR spectroscopy was performed on a Bruker AVANCE 400 MHz NMR spectrometer (Bruker Instrument Co., Ltd., Switzerland). Mass spectra (EIS) were recorded by Q-Exactive quadrupole mass spectrometer (Thermo Fisher Scientific Inc.). UV-vis spectra were recorded by T6 New Century UV spectrophotometer (Beijing Purkinje General Instrument Co., Ltd, Beijing, China). The photoluminescence spectra and time-resolved emission spectra were collected using an Edinburgh FL1000 Fluorometer (Edinburgh Instruments Ltd., England). Absolute quantum yields were determined by the integrating sphere (142 mm in diameter) using Edinburgh FLS1000 spectrofluorophotometer.

### Synthesis of 5-(4-aminophenyl)-10,15,20-triphenyl porphine (ATPP)

Tetraphenylporphyrin (1.29 g, 2.1 mmol) was dissolved in trifluoroacetic acid (20 mL) and stirred at 0 °C for 10 min.  $NaNO_2$  (180 mg, 2.6 mmol) was added in three portions and the mixture was further reacted at 0 °C for 30 min. Then, the reaction was quenched by adding 100 mL of deionized water and extracted several times with dichloromethane. The combined organic phases were washed with saturated aqueous solution of  $NaHCO_3$ . The separated organic phase was dried over anhydrous  $Na_2SO_4$  and concentrated under vacuum to get the crude product NTPP. Under argon, the crude product NTPP was dissolved in concentrated HCl (40 mL) and  $SnCl_2 \cdot 2H_2O$  (1.08 g, 4.8 mmol) was added. The mixture was stirred at 65 °C for 6 h. After the completion of the reaction, 20% NaOH solution was added to quench the system to neutral. The mixture was extracted three times with

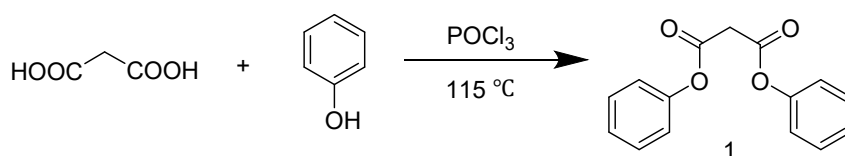
dichloromethane (50 mL × 3). The separated organic phase was dried with anhydrous MgSO<sub>4</sub> and removed under reduced pressure. The crude product was purified by column chromatography (petroleum ether/ethyl acetate = 4/1) to obtain ATPP (55 mg). MS: *m/z* = 630.26 [M]<sup>+</sup>. <sup>1</sup>H NMR (400 MHz, CDCl<sub>3</sub>) δ 8.93 (d, *J* = 2.8 Hz, 2H), 8.83 (s, 6H), 8.22 (d, *J* = 6.4 Hz, 6H), 8.00 (d, *J* = 7.7 Hz, 2H), 7.76 (m, 9H), 7.07 (d, *J* = 7.9 Hz, 2H), 4.03 (s, 2H, -NH<sub>2</sub>), -2.84 (s, 2H, N-H). <sup>13</sup>C NMR (151 MHz, CDCl<sub>3</sub>) δ 146.01, 142.30, 142.25, 135.69, 134.57, 132.35, 130.92, 129.51, 128.86, 127.66, 126.68, 126.67, 120.91, 120.00, 119.77, 113.43.



**Scheme S1.** Preparation of ATPP.

### Synthesis of diphenyl malonate (1)

POCl<sub>3</sub> (6 mL) was added dropwise to a mixture of malonic acid (5.20 g, 50 mmol) and phenol (9.40 g, 100 mmol) at 0 °C. The mixture was heated at 115 °C for 2 h. After cooled to room temperature, the upper layer was poured into 150 mL of deionized water and extracted with EtOAc three times. The separated organic phase was dried with anhydrous Na<sub>2</sub>SO<sub>4</sub> and removed under reduced pressure, resulting in a pale-yellow viscous liquid. After standing for several hours, pale-yellow needle-shaped crystals were obtained (9.80 g, 76% yield).

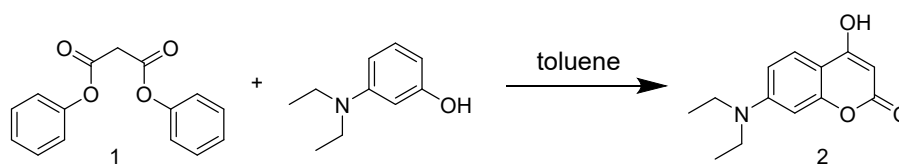


**Scheme S2.** Preparation of diphenyl malonate.

### Synthesis of 7-diethylamino-4-hydroxycoumarin (2)

To a solution of diphenyl malonate (9.23 g, 36 mmol) in anhydrous toluene (50 mL), 3-(N, N-diethylamino)phenol (5.95 g, 36 mmol) was added. The reaction mixture was heated to 115 °C for 10 h. After the completion of the reaction, the mixture was filtered and washed with n-hexane to obtain a pale-yellow solid product (6.10 g, 72% yield). <sup>1</sup>H NMR (400 MHz, DMSO) δ 11.91 (s, 1H), 7.54 (s, 1H), 6.66 (d, *J* = 8.9 Hz, 1H), 6.45 (t, *J* = 2.0 Hz, 1H), 5.24 (s, 1H), 3.40 (m, *J* = 5.5 Hz,

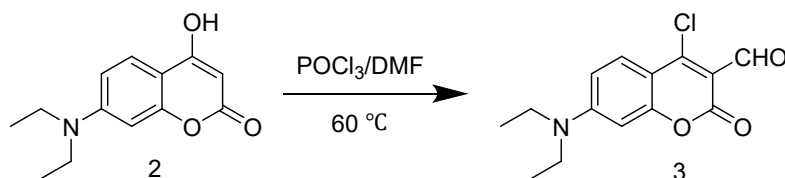
4H), 1.12 (t,  $J = 7.0$  Hz, 6H).



**Scheme S3.** Preparation of 7-diethylamino-4-hydroxycoumarin.

### Synthesis of 4-chloro-7-diethylaminocoumarin-3-aldehyde (3)

Anhydrous DMF (1.4 mL) was added dropwise to  $\text{POCl}_3$  (1.4 mL) under nitrogen at room temperature and stirred for 30 min to give a pink solution (formylating reagent). Then, 7-(diethylamino)-4-hydroxycoumarin (1.17 g, dissolved in 6.6 mL DMF) was added dropwise to the above solution while stirring continuously, resulting in a scarlet suspension. The mixture was stirred at 60 °C for 12 h and then poured into 100 mL of ice water. NaOH solution (20%) was added to adjust the pH of the mixture to 5, resulting in a large amount of precipitate. The crude product was filtered while being washed with distilled water and then dried in vacuum to obtain orange solid (1.01 g, 72% yield). MS:  $m/z = 280.07$   $[\text{M}]^+$ .  $^1\text{H}$  NMR (400 MHz,  $\text{CDCl}_3$ )  $\delta$  10.3 (s, 1H), 7.82 (d,  $J = 9.3$  Hz, 1H), 6.93 (m,  $J = 9.4$  Hz, 2.5, 1H), 6.49 (d,  $J = 2.4$  Hz, 1H), 3.53 (m,  $J = 7.1$  Hz, 4H), 1.16 (t,  $J = 7.1$  Hz, 6H).  $^{13}\text{C}$  NMR (151 MHz,  $\text{CDCl}_3$ )  $\delta$  186.98, 159.91, 156.41, 154.00, 153.59, 129.25, 111.02, 110.54, 107.70, 96.63, 45.33, 12.42.

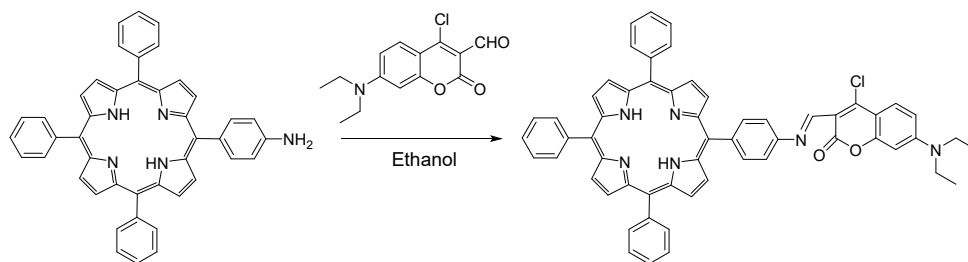


**Scheme S4.** Preparation of 4-chloro-7-diethylaminocoumarin-3-aldehyde.

### Synthesis of ATPP-Cou

Under nitrogen, the compound 3 (28 mg) was dissolved in EtOH (20 mL). And, ATPP (75.6 mg) in toluene (20 mL) was added dropwise. The reaction mixture was stirred at 78 °C for 24 h and then the solvent was removed under reduced pressure. The crude product was purified by column chromatography (petroleum ether/ethyl acetate=3/1) to afford ATPP-Cou (43 mg, 41% yield). MS:  $m/z = 855.34$   $[\text{M}-\text{Cl}]^+$ .  $^1\text{H}$  NMR (400 MHz,  $\text{CDCl}_3$ )  $\delta$  9.34 (s, 1H), 8.86 (m, 8H), 8.74 (m, 3H), 8.47 (d,  $J = 6.6$  Hz, 1H), 8.22 (m, 6H), 7.77 (m, 10H), 6.83 (d,  $J = 11.4$  Hz, 1H), 6.63 (d,  $J = 2.3$  Hz, 1H), 3.53 (d,  $J = 7.0$  Hz, 4H), 1.31 (t,  $J = 7.1$  Hz, 6H), -2.82 (s, 2H).  $^{13}\text{C}$  NMR (151 MHz,  $\text{CDCl}_3$ )  $\delta$  167.82, 162.26, 154.93, 151.34, 151.07, 142.10, 142.06, 141.56, 140.03, 139.36, 134.61, 134.42,

130.93, 128.85, 127.83, 126.77, 126.51, 125.29, 120.65, 120.51, 118.17, 115.72, 109.27, 107.49, 98.04, 44.89, 12.64.



**Scheme S5.** Preparation of ATPP-Cou.

### Electrochemistry and ECL detection

ECL signals were measured with a model MPI-E electrochemiluminescence analyzer (Xi'an Remax Electronic Science & Technology Co. Ltd., China). The photomultiplier tube (PMT) voltage was set at 800 V. A typical three-electrode system (a glassy carbon electrode, a Pt coil electrode, an Ag/AgCl electrode as working electrode, counter electrode, and reference electrode, respectively) was used for electrochemistry and ECL experiments.

### IMPS and SPECM measurement

Intensity modulated photocurrent spectroscopy (IMPS) was performed in a frequency range of 1-10000 Hz. A monochromatic LED light of 470 nm (100 mW cm<sup>-2</sup>) was used as the incident light source. The resulting photocurrent response was recorded under a constant applied bias. The charge-transfer time ( $\tau_d$ ) of photoanode was calculated according to  $\tau_d=1/(2\pi f_{min})$ . SPECM measurements were performed at self-established platform with four-electrode system. Pt wire and Ag/AgCl (saturated KCl) are utilized as the auxiliary electrode and reference electrode, respectively. The ultramicroelectrode (UME) with a diameter of 25  $\mu\text{m}$  and substrate electrodes modified by ATPP or ATPP-Cou were designated as working electrode 1 and working electrode 2, respectively. All experiments were conducted at room temperature under the aforementioned illumination source. The potential of the UMEs and substrate electrode was set at 0.0 V and 0.2 V vs Ag/AgCl, respectively, throughout the measurement process. The feedback mode was employed to study the kinetics, where  $\text{K}_3\text{Fe}(\text{CN})_6$  in 100 mM KCl (aq) served as a probe molecule to investigate the electrochemical properties. Referring to the experimental simulation conducted in our previous study, the rate constant ( $K_{\text{eff}}$ ) can be determined.

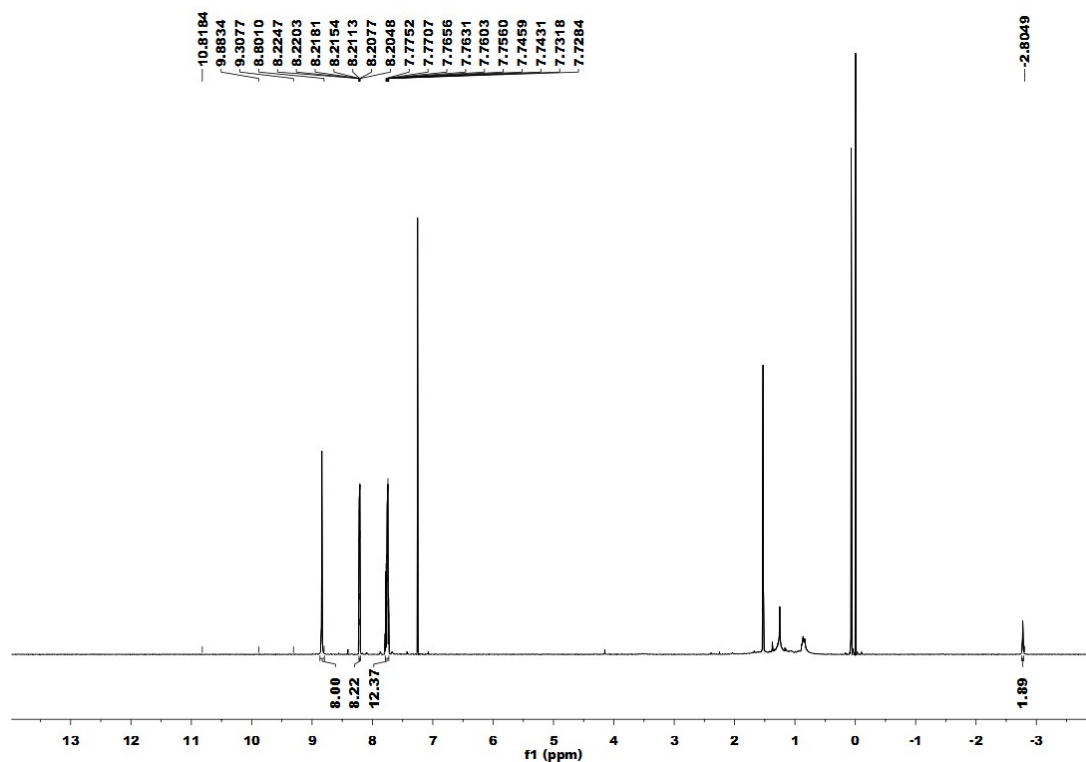


Figure S1. The  $^1\text{H}$  NMR spectrum of TPP ( $\text{CDCl}_3$ ).

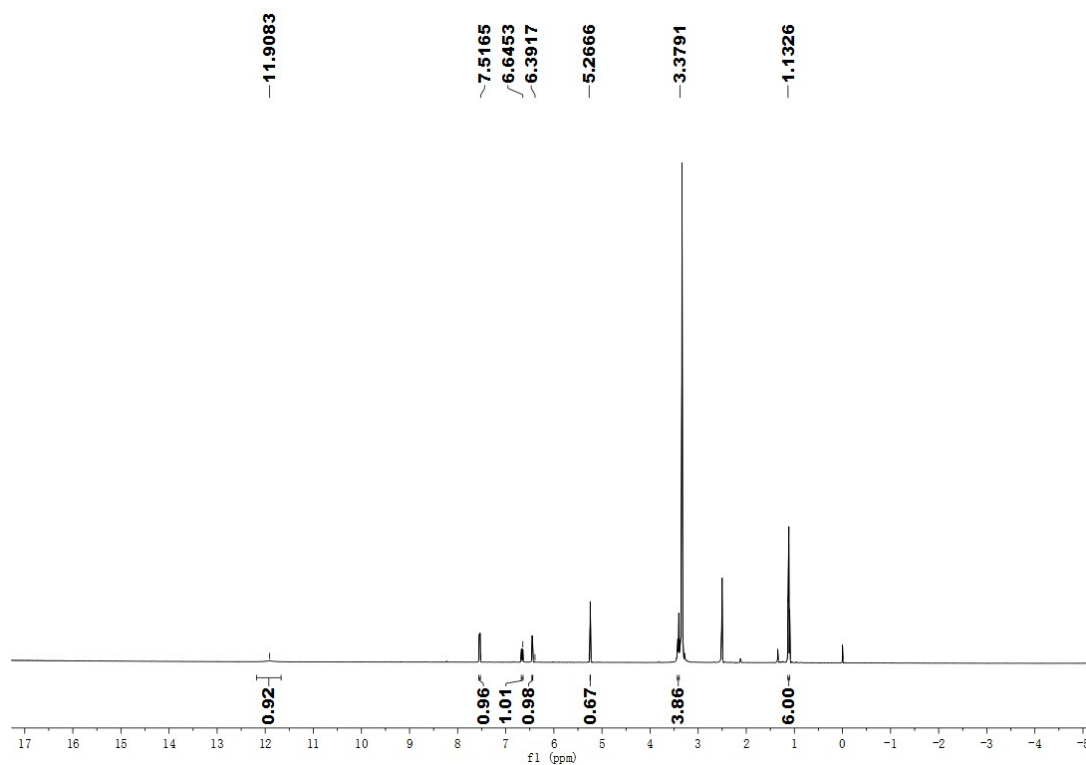
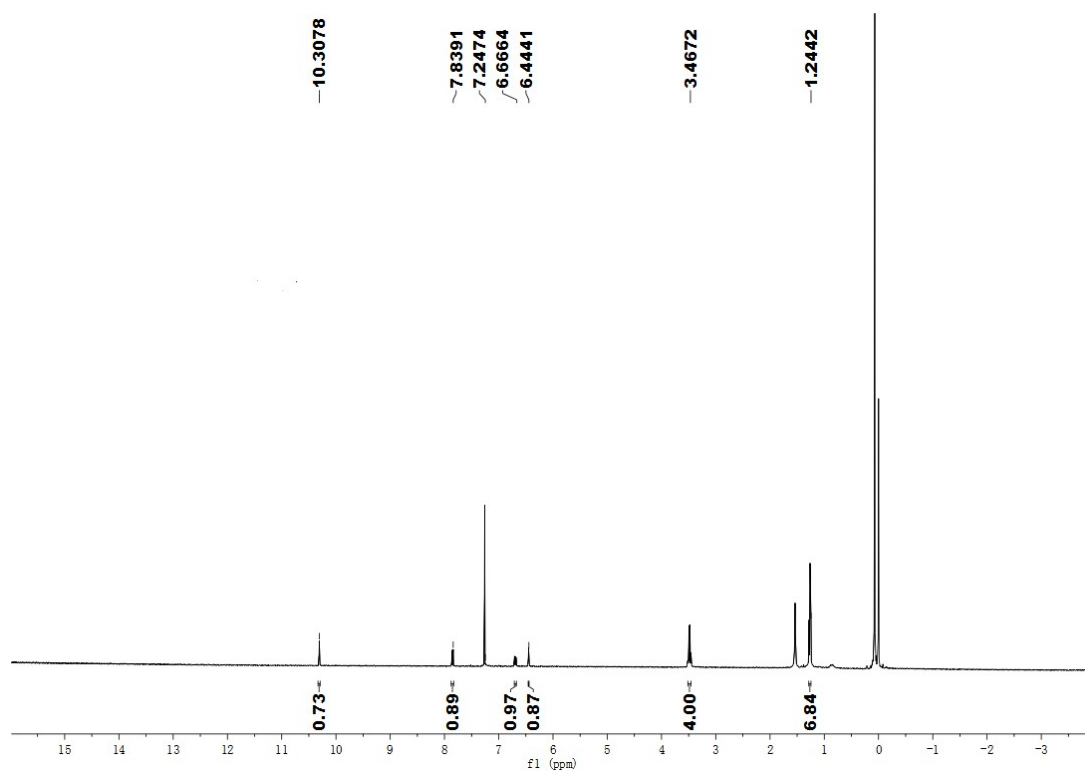
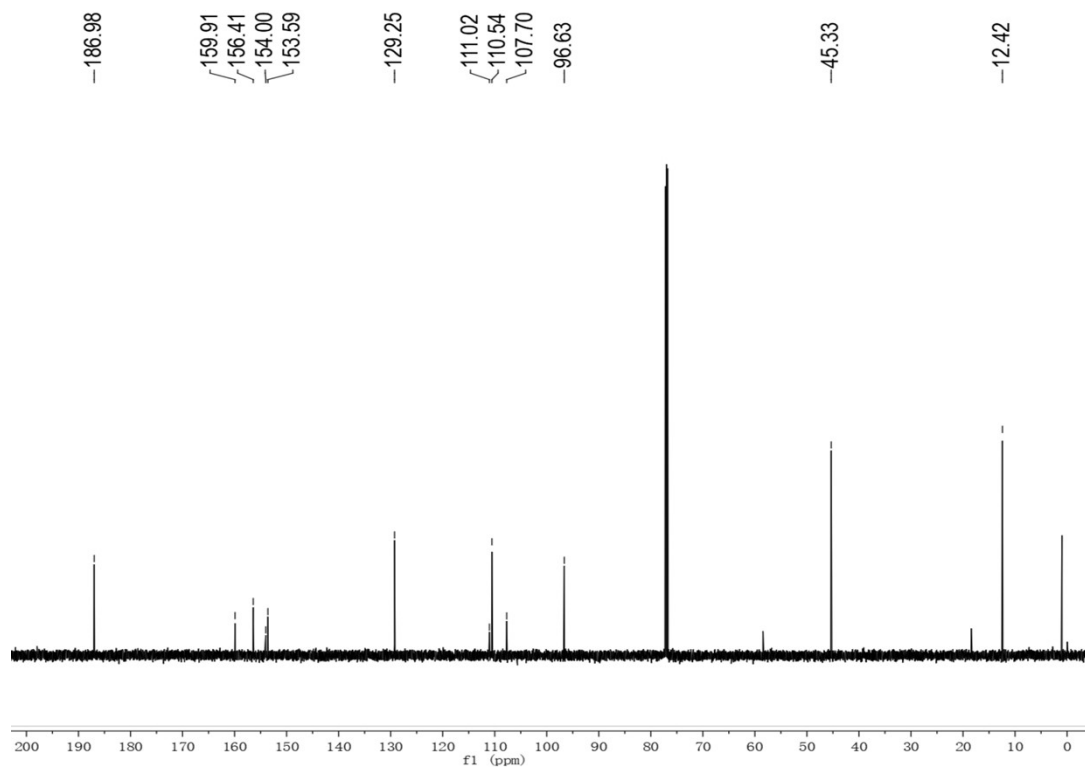


Figure S2. The  $^1\text{H}$  NMR spectrum of 7-diethylamino-4-hydroxycoumarin ( $\text{DMSO-D}_6$ ).



**Figure S3.** The  $^1\text{H}$  NMR spectrum of 4-chloro-7-diethylaminocoumarin-3-aldehyde ( $\text{CDCl}_3$ ).



**Figure S4.** The  $^{13}\text{C}$  NMR spectrum of 4-chloro-7-diethylaminocoumarin-3-aldehyde ( $\text{CDCl}_3$ ).



LXQ-WANGYALI-1 #127-165 RT: 0.56564-0.73501 AV: 39 NL: 8.58E7  
T: FTMS + p ESI Full lock ms [50.0000-750.0000]

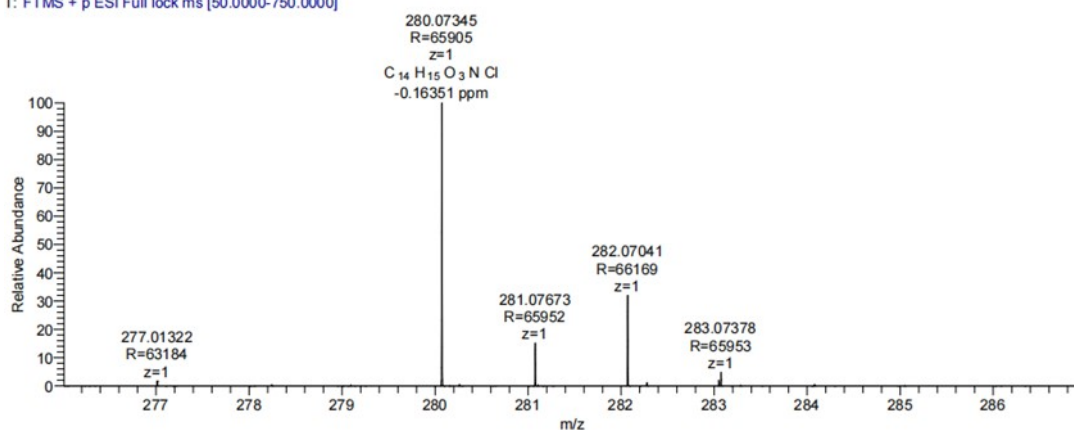


**Figure S5.** The mass spectrum (ESI) of 4-chloro-7-diethylaminocoumarin-3-aldehyde. MS: m/z = 280.07 [M]<sup>+</sup>.

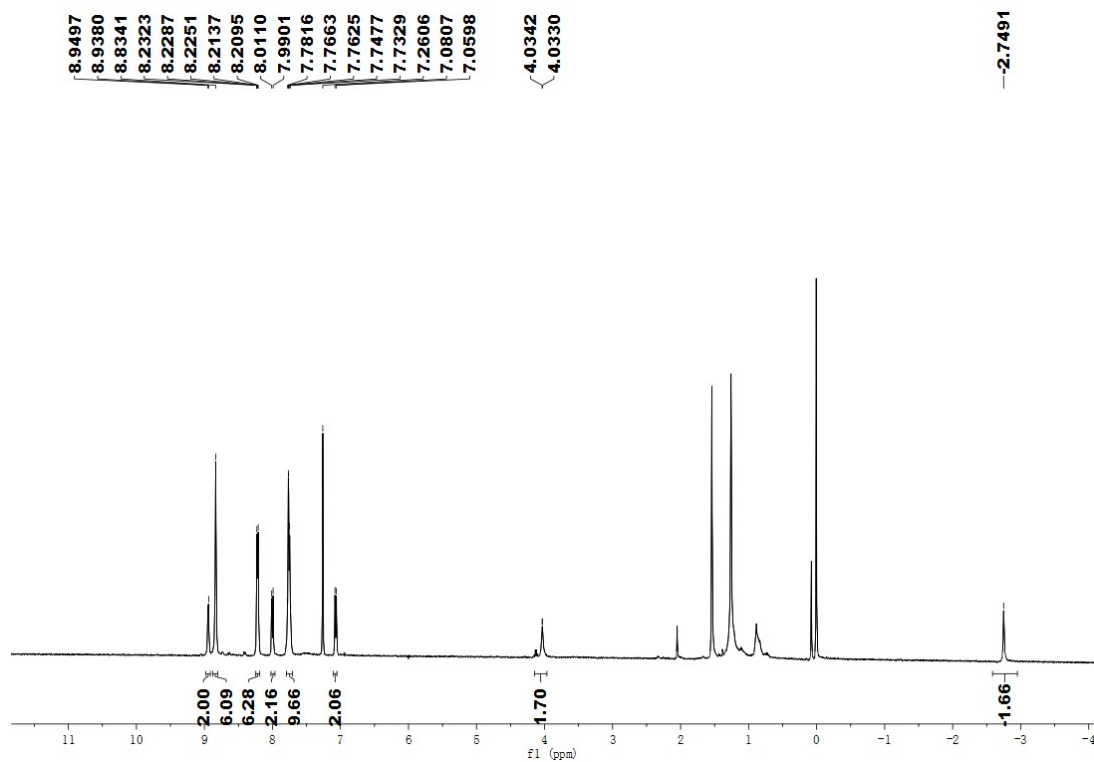


**Figure S6.** The <sup>1</sup>H NMR spectrum of 5-(4-aminophenyl)-10,15,20-triphenylporphyrin (ATPP) (CDCl<sub>3</sub>).

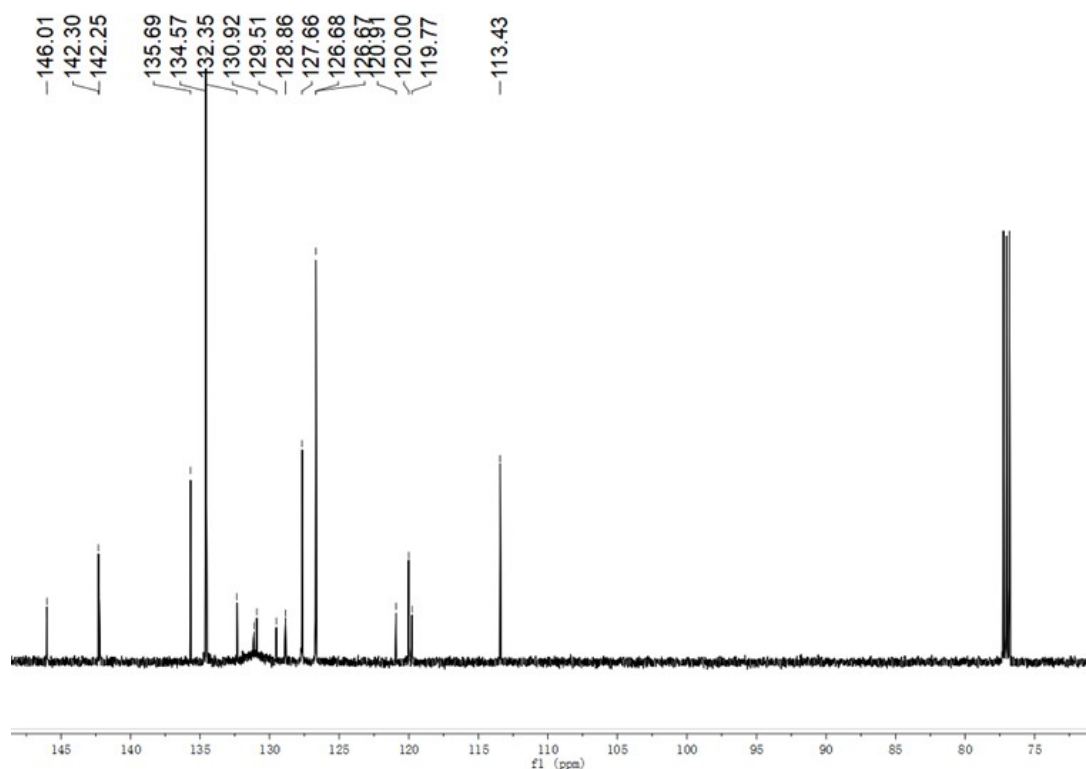


**Figure S7.** The  $^{13}\text{C}$  NMR spectrum of 5-(4-aminophenyl)-10,15,20-triphenylporphyrin (ATPP) ( $\text{CDCl}_3$ ).

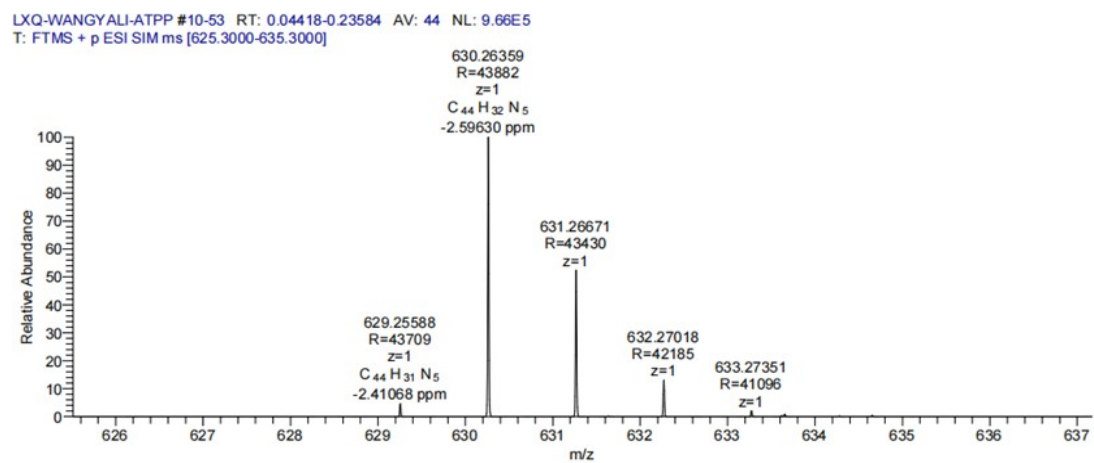


**Figure S8.** The mass spectrum (ESI) of 5-(4-aminophenyl)-10,15,20-triphenylporphyrin (ATPP). MS:  $m/z = 630.26$   $[\text{M}]^+$ .

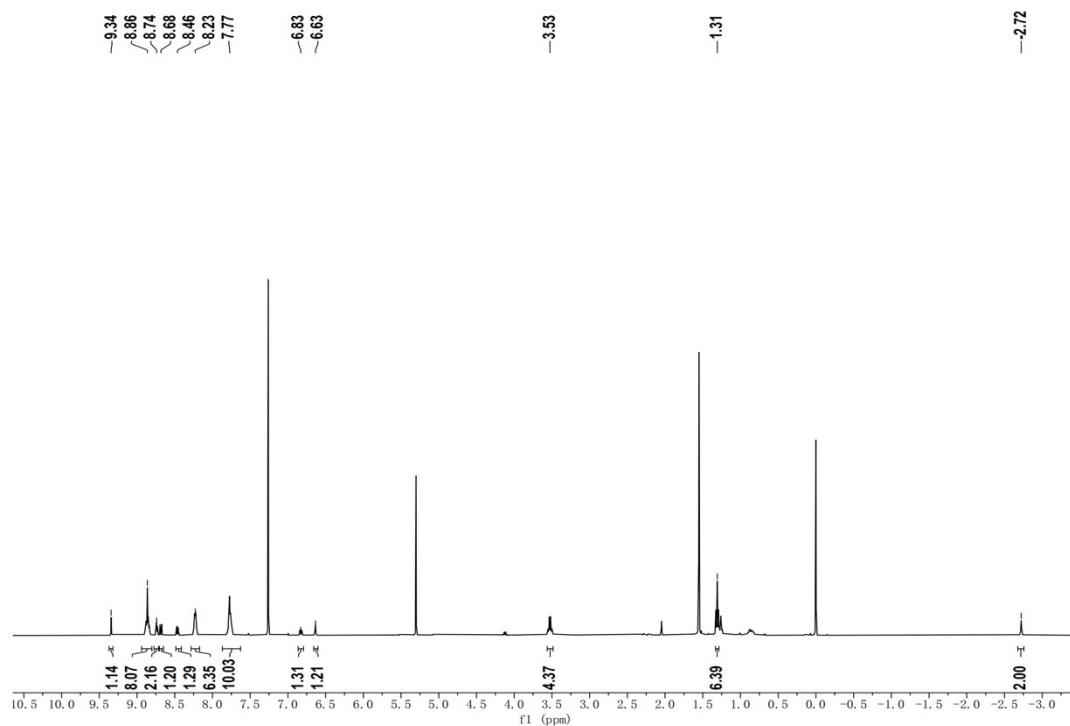


**Figure S9.** The  $^1\text{H}$  NMR spectrum of ATPP-Cou ( $\text{CDCl}_3$ ).

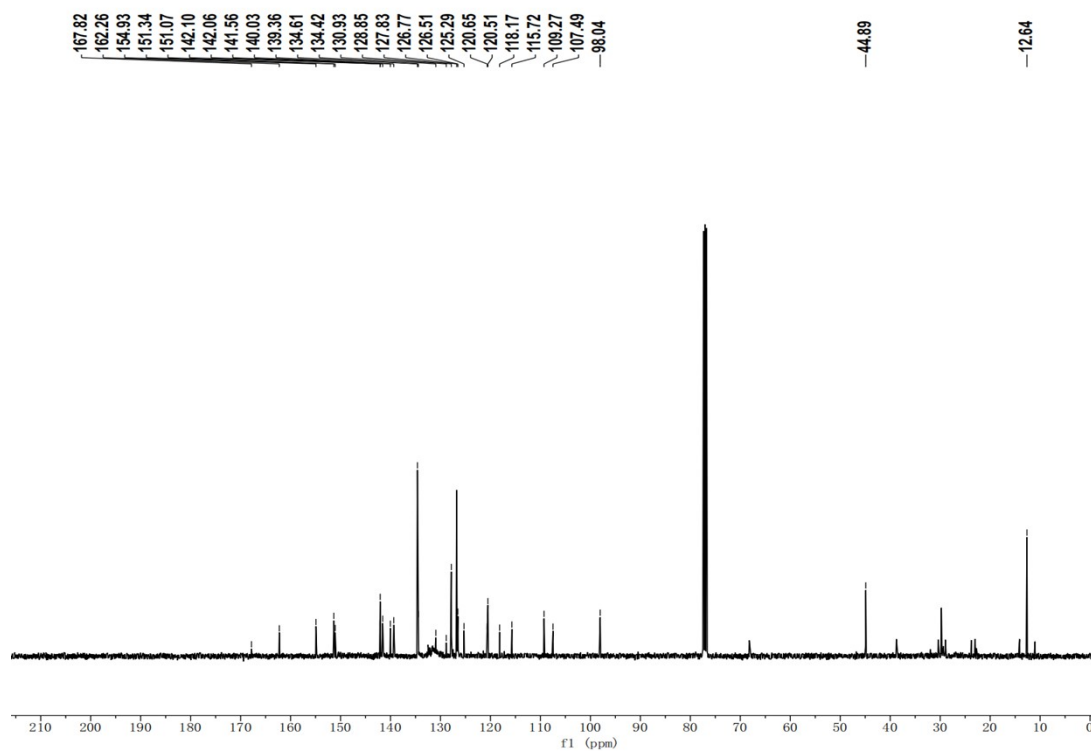


**Figure S10.** The  $^{13}\text{C}$  NMR spectrum of ATPP-Cou ( $\text{CDCl}_3$ ).

LXQ-WANGYALI-W1 #41-101 RT: 0.18234-0.44976 AV: 61 NL: 6.72E7  
T: FTMS + p ESI Full lock ms [80.0000-1200.0000]

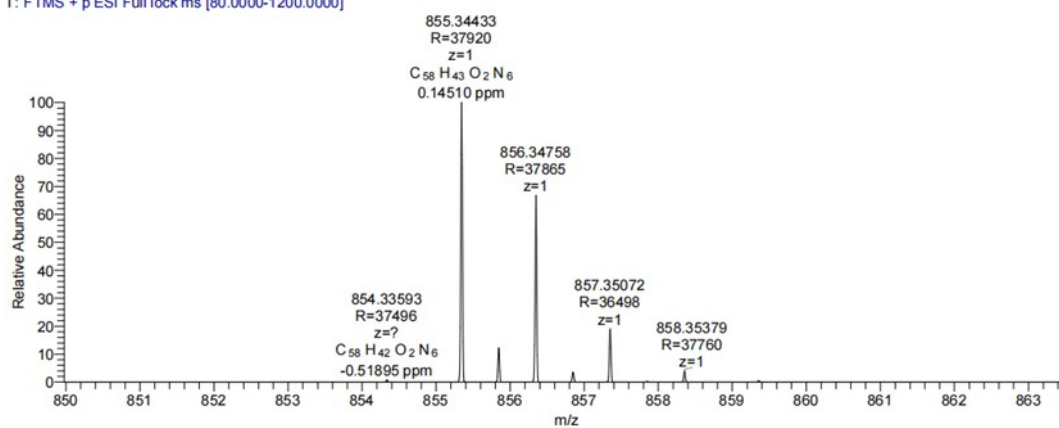


**Figure S11.** The mass spectrum (ESI) of ATPP-Cou. MS:  $m/z = 855.34 [M-Cl]^+$ .

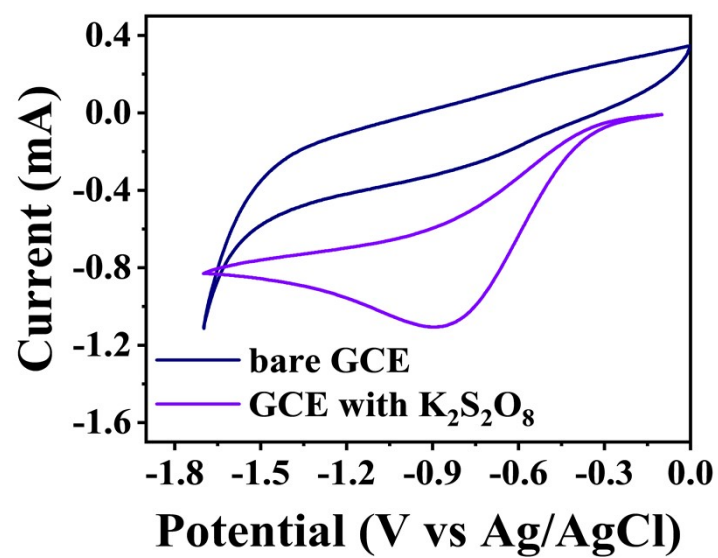


**Figure S12.** CV curves of the bare GCE in PBS with (purple line) and without (navy-blue line)  $K_2S_2O_8$ .

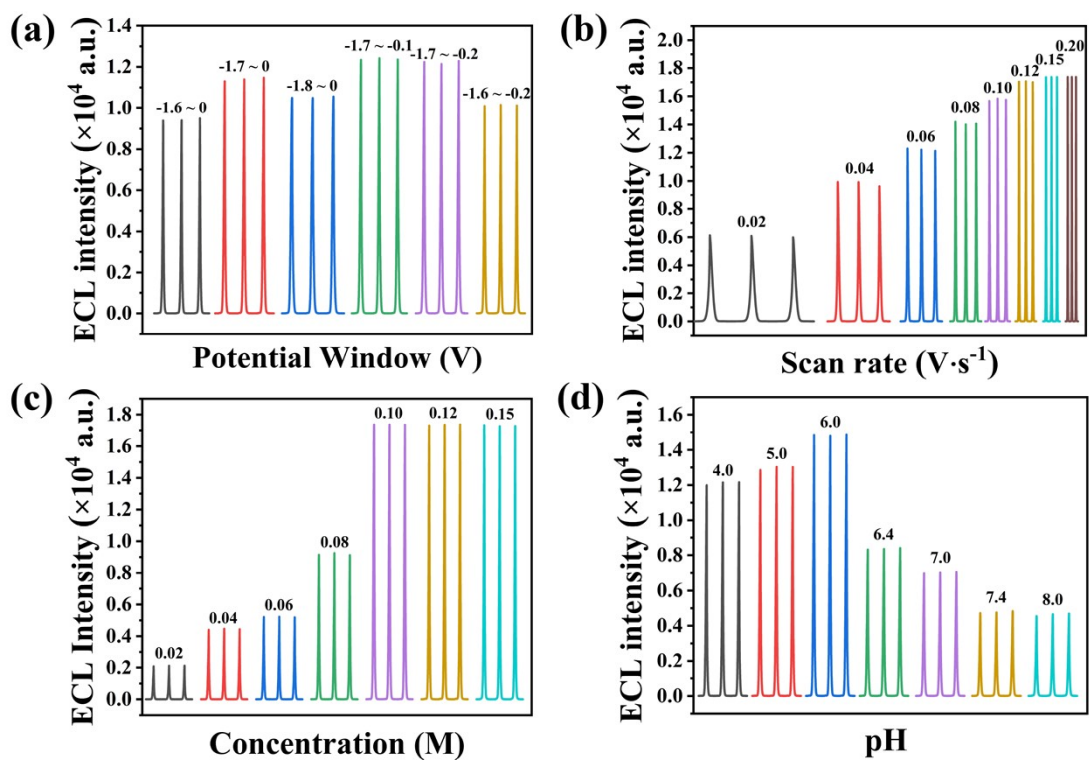


**Figure S13.** Effect of different experimental conditions on the ECL system: (a) different potential windows, (b) different scan rates, (c) different concentrations of  $K_2S_2O_8$ , and (d) different pH values.

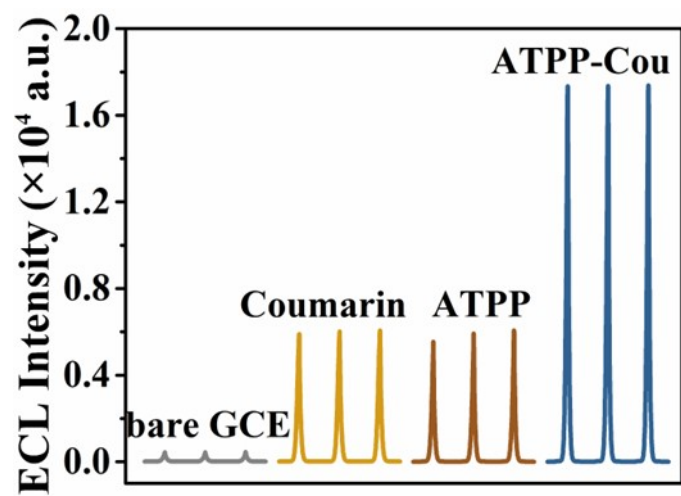


**Figure S14.** ECL intensity of the studied systems (bare GCE, Coumarin, ATPP and ATPP–Cou).

**Table S1.**  $K_{\text{eff}}$  values of different samples

Sample	ATPP	ATPP-Cou
$K_{\text{eff}}(10^{-2} \text{ cm} \cdot \text{s}^{-1})$	9.78	8.38

**Table S2.** Transit time values of different samples

Sample	ATPP	ATPP-Cou
$f_{\text{IMPS}}(\text{Hz})$	208.93	69.183
$\tau_d(\text{ms})$	0.76	2.30

**Table S3.** The fluorescence lifetime fitting data of coumarin, ATPP and ATPP-Cou

Compound	$\tau_1(\text{ns})$	$A_1$	$\tau_2(\text{ns})$	$A_2$	$\tau_{\text{avg}}(\text{ns})$	$R^2$
Coumarin	0.59	2462.01	2.86	392.59	1.60	0.9957
ATPP	4.73	323.3	2.47	1746.28	3.06	0.9988
ATPP-Cou	9.13	977.23	/	/	9.13	1.0085

$$\tau_{\text{avg}} = \frac{\sum_n A_n \tau_n^2}{\sum_n A_n \tau_n}$$

The average decay times ( $\tau_{\text{avg}}$ ) were calculated as follow:

**Table S4.** Comparison of the reported methods for  $\text{Cu}^{2+}$  detection

Material	Detection method	Linear range (nM)	LOD (nM)	Ref.
TSPP	ECL	5.0–160	1.56	[1]
g-C <sub>3</sub> N <sub>4</sub>	ECL	2.5–100	0.90	[2]
Ni/NiO/ZnO/Chitosan wire	EC	0–6000	0.81	[3]
ZIF-67@GO-2	EC	60–20000	69	[4]
polyethyleneimine decorated black phosphorus	EC	250–177000	20	[5]
CCYWDAHRDY-AuNCs	FL	100–4200	52	[6]



ATPP–Cou	ECL	10–385	0.64	This Work
----------	-----	--------	------	-----------

**Table S5.** Spiked recovery tests for river water samples

Sample	Added (nM)	Found (nM)	Recovery (%)	RSD (%)
Yellow River	15.00	14.33	100.2	4.85
		14.73		
	55.00	16.03	98.6	1.86
		55.24		
	75.00	52.83	96.9	1.52
		54.69		
		72.45		
		71.37		
		74.13		

## References

- [1] Zhang, J., Devaramani, S., Shan, D., Lu, X. Electrochemiluminescence behavior of *meso*-tetra(4-sulfonatophenyl)porphyrin in aqueous medium: its application for highly selective sensing of nanomolar Cu<sup>2+</sup>. *Anal. Bioanal. Chem.* **2016**, 408(25), 7155-7163.
- [2] Cheng, C., Huang, Y., Tian, X., Zheng, B., Li, Y., Yuan, H., Xiao, D., Xie, S., Choi, M. M. F. Electrogenated chemiluminescence behavior of graphite-like carbon nitride and its application in selective sensing Cu<sup>2+</sup>. *Anal. Chem.* **2012**, 84(11), 4754-4759.
- [3] Yu, J., Zhang, X., Zhao, M., Ding, Y., Li, Z., Ma, Y., Li, H., Cui, H. Fabrication of the Ni-based composite wires for electrochemical detection of copper(II) ions. *Anal. Chim. Acta* **2021**, 1143, 45-52.
- [4] Xu, Y., Sun, L., Sun, Y., Liu, B., Guo, H., Wei, Y., Feng, H., Wei, Y., Zhang, X. Effect of heat treatment on sensing performance of ZIF-67@GO for the detection of copper ions. *Colloids Surf., A* **2022**, 649, 129500.
- [5] Li, Y., Shi, Z., Zhang, C., Wu, X., Liu, L., Guo, C., Li, C. M. Highly stable branched cationic polymer-functionalized black phosphorus electrochemical sensor for fast and direct ultratrace detection of copper ion. *J. Colloid Interf. Sci.* **2021**, 603, 131-140.
- [6] Zhuang, H., Jiang, X., Wu, S., Wang, S., Pang, Y., Huang, Y., Yan, H. A novel polypeptide-modified fluorescent gold nanoclusters for copper ion detection. *Sci. Rep.* **2022**, 12(1), 6624.

